



ORIGINAL ARTICLE

Metastatic ability and the epithelial-mesenchymal transition in induced cancer stem-like hepatoma cells

Mitsuo Nishiyama¹ | Ryouichi Tsunedomi¹  | Kiyoshi Yoshimura² |
 Noriaki Hashimoto¹ | Satoshi Matsukuma¹ | Hiroyuki Ogihara³ | Shinsuke Kanekiyo¹ |
 Michihisa Iida¹ | Kazuhiko Sakamoto¹ | Nobuaki Suzuki¹ | Shigeru Takeda¹ |
 Shigeru Yamamoto¹ | Shigefumi Yoshino⁴ | Tomio Ueno⁵ | Yoshihiko Hamamoto³ |
 Shoichi Hazama⁶  | Hiroaki Nagano¹

¹Department of Gastroenterological, Breast and Endocrine Surgery, Yamaguchi University Graduate School of Medicine, Ube, Japan

²Division of Cancer Immunotherapy, Exploratory Oncology Research and Clinical Trial Center, National Cancer Center, Tokyo, Japan

³Division of Electrical, Electronic and Information Engineering, Yamaguchi University Graduate School of Sciences and Technology for Innovation, Ube, Japan

⁴Oncology Center, Yamaguchi University Hospital, Ube, Japan

⁵Department of Digestive Surgery, School of Medicine, Kawasaki Medical School, Kurashiki, Japan

⁶Department of Translational Research and Developmental Therapeutics against Cancer, Yamaguchi University Faculty of Medicine, Ube, Japan

Correspondence

Ryouichi Tsunedomi, Department of Gastroenterological, Breast and Endocrine Surgery, Yamaguchi University Graduate School of Medicine, Ube, Yamaguchi, Japan. Email: tsune-r@yamaguchi-u.ac.jp

Funding information

Japan Society for the Promotion of Science (KAKENHI grant nos. 16K10574, 25861192, and 24659610).

Cancer stem cells (CSCs) are thought to play important roles in cancer malignancy. Previously, we successfully induced sphere cancer stem-like cells (CSLCs) from several cell lines and observed the property of chemoresistance. In the present study, we examined the metastatic potential of these induced CSLCs. Sphere cancer stem-like cells were induced from a human hepatoma cell line (SK-HEP-1) in a unique medium containing neural survival factor-1. Splenic injection of cells into immune-deficient mice was used to assess hematogenous liver metastasis. Transcriptomic strand-specific RNA-sequencing analysis, quantitative real-time PCR, and flow cytometry were carried out to examine the expression of epithelial-mesenchymal transition (EMT)-related genes. Splenic injection of CSLCs resulted in a significantly increased frequency of liver metastasis compared to parental cancer cells ($P < .05$). In CSLCs, a mesenchymal marker, Vimentin, and EMT-promoting transcription factors, Snail and Twist1, were upregulated compared to parental cells. Correspondingly, significant enrichment of the molecular signature of the EMT in CSLCs relative to parental cancer cells was shown ($q < 0.01$) by RNA-sequencing analysis. This analysis also revealed differential expression of CD44 isoforms between CSLCs and parental cancer cells. Increasing CD44 isoforms containing an extra exon were observed, and the standard CD44 isoform decreased in CSLCs compared to parental cells. Interestingly, another CD44 variant isoform encoding a short cytoplasmic tail was also upregulated in CSLCs (11.7-fold). Our induced CSLCs possess an increased liver metastatic potential in which promotion of the EMT and upregulation of CD44 variant isoforms, especially short-tail, were observed.

KEYWORDS

cancer stem cell, CD44v, EMT, hepatoma, intrahepatic metastasis

1 | INTRODUCTION

Cancer stem cells (CSCs) have been defined as a small subset of cancer cells within the tumor bulk that show potential causes of malignant properties of tumors, such as tumor initiation, metastasis, recurrence, and chemoresistance.^{1,2} Expression of various CSC markers such as CD44, CD133, CD90, CD13, aldehyde dehydrogenase, and epithelial cell adhesion molecules has been identified by recent research in many solid carcinomas, suggesting a relationship with poor prognosis.³⁻⁷ It was also reported that plasticity enables differentiated cancer cells to transform into cells harboring cancer stem-like properties through the epithelial-mesenchymal transition (EMT).^{8,9} Based on this concept, we have successfully induced cancer stem-like cells (CSLCs) from several cell lines using a unique medium supplemented with neural survival factor-1.¹⁰⁻¹² The obtained sphere CSLCs have increased resistance to several anticancer drugs.¹²

Metastasis is a life-threatening systemic condition of all cancer patients. Hepatoma patients have an especially poor prognosis due to intrahepatic recurrence even after most potentially curative therapies such as surgical resection and liver transplantation.¹³⁻¹⁵ Only a small fraction of cancer cells that survive in the systemic circulation are able to give rise to clinically relevant metastases.¹⁶ These cells are considered CSCs and have an enhanced capacity for metastatic behavior *in vitro* and *in vivo*.¹⁷⁻¹⁹

In this study, we evaluated the metastatic ability of our CSLCs by splenic injection into immune-deficient mice, and further examined metastatic potential-related features in the induced CSLCs.

2 | MATERIALS AND METHODS

2.1 | Cell lines

The human hepatoma SK-HEP-1 and HuH-7 cell lines were purchased from ATCC (Rockville, MD, USA) and the Health Science Research Resources Bank (Osaka, Japan). The SK-HEP-1 and HuH-7 cell lines are from poorly and well differentiated hepatomas, respectively. Cells were cultured in DMEM (Nissui Pharmaceutical, Tokyo, Japan) containing 10% heat-inactivated FBS (Thermo Fisher Scientific, Kanagawa, Japan), penicillin (100 U/mL), streptomycin (100 µg/mL), and sodium bicarbonate (1.5 g/L) at 37°C in a humidified atmosphere of 5% CO₂ in air.

2.2 | Induction of sphere cells

Cells were suspended in the sphere induction medium, which was based on neural stem cell medium.¹² This medium contained 2 µg/mL heparin (Sigma-Aldrich Japan, Tokyo, Japan), 10 ng/mL human recombinant epidermal growth factor (Sigma-Aldrich), 10 ng/mL basic fibroblast growth factor (Merck Millipore, Tokyo, Japan), 10 ng/mL leukemia inhibitory factor (Merck Millipore), 60 µg/mL N-acetyl-L-cysteine (Sigma-Aldrich), and 1/50 volume neural survival factor-1 (Lonza, Tokyo, Japan) to induce floating sphere cells.

2.3 | Splenic injection of tumor cells

NOD-Rag1^{null} IL2r^{null} double mutant mice (NRG mice) were purchased from the Jackson Laboratory (Bar Harbor, ME, USA) and maintained in a HEPA-filtered environment with autoclave-sterilized cages, food, and bedding. Paraffin-embedded liver tissues were stained with H&E; thereafter, images of whole sections were obtained using a BZ-X700 microscope (Keyence, Osaka, Japan). The proportion of tumor areas was calculated using the BZ-X Analyzer (Keyence). All animal studies were carried out in accordance with the Institutional Animal Care and Use Committee of Yamaguchi University (Ube, Japan) and conformed to the Guide for the Care and Use of Laboratory Animals published by the US NIH (Bethesda, MD, USA).

The ability of SK-HEP-1 and SK-sphere cells to produce tumor nodules in the liver was studied subsequent to their implantation into the spleen of 8-12-week-old NRG female mice. Mice were anesthetized by inhalation of 2% isoflurane in oxygen and placed in the supine position. A small abdominal incision was made in the left flank and the spleen was exposed. Viable tumor cells (10³ or 10⁴) in 0.1 mL Hanks' balanced salt solution (Thermo Fisher Scientific) were injected into the spleen by a 27-gauge needle and the spleen was then resected. The wound was closed in one layer with metal wound clips. After 8 weeks, injected mice were killed and necropsied.

2.4 | RNA sequencing

SK-HEP-1 and SK-sphere cells were lysed with TRIzol (Thermo Fisher Scientific). Total RNAs were isolated with the miRNeasy Mini Kit (Qiagen, Tokyo, Japan). RNA quality was assured by Bioanalyzer analysis (Agilent Technologies, Tokyo, Japan). Sequencing libraries were constructed using the TruSeq Stranded Total RNA with RiboZero Gold LT Sample Prep kit (Illumina, Tokyo, Japan) according to manufacturer's instructions. Libraries were pooled after quantification by Bioanalyzer analysis as well as fluorometrically using Qubit dsDNA HS Assay kits and a Qubit 2.0 Fluorometer (Thermo Fisher Scientific). Sequencing of paired-end fragments (75 bp × 2) was carried out on a NextSeq 500 sequencing platform (Illumina) to a depth, in triplicate, of 123-150 million fragments for SK-HEP-1 and SK-sphere cells, and a depth, in duplicate, of 42-46 million fragments for HuH-7 cells.

Data for each sample were separated using unique barcode combinations and to generate FASTQ files. Next-generation sequencing data were subjected to reads cleaning with cutadapt (version 1.8.3)²⁰ and cmpfastq_pe.pl (http://compbio.brc.iop.kcl.ac.uk/software/cmpfastq_pe.php). After a quality control step, the filtered short reads were mapped to the reference genome (hg38) with STAR (version 2.5.1b) 2-pass mapping.²¹ Strand-specific counts of fragments from each sample were normalized with the trimmed mean of M values method²² using the TCC package.^{23,24} Differentially expressed genes were identified based on a false discovery rate *q*-value threshold of <0.05. Genes were considered differentially expressed when

displaying a change of more than two-fold with a q -value of <0.05 . Gene set enrichment analysis was carried out with Java command line program GSEA2 (version 2.2.1).²⁵

2.5 | Quantification of CD44 isoforms expression

Because we obtained more than 100 million paired-ends in the RNA-sequencing (RNA-seq) analysis with SK-HEP-1 and SK-sphere cells, we evaluated the expression of each CD44 isoform. Isoform quantification was accomplished by the Cuffdiff program in Cufflinks (version 2.2.1)²⁶ with BAM files generated from the STAR program.

2.6 | Flow cytometry

After cell cultivation, sphere and parental adherent cells were dissociated with Accumax and Accutase (Innovative Cell Technologies, San Diego, CA, USA), respectively. Dissociated cells were stained with Fixable Viability Dye eFluor 450 (Thermo Fisher Scientific) to distinguish between living and dead cells. For flow cytometric analyses, cells were incubated with the following fluorescence-conjugated antibodies: anti-Vimentin phycoerythrin (PE) (MAB4527; Abnova, Taipei, Taiwan) and anti-epithelial cell adhesion molecule (EpCAM) FITC (130-080-301; Miltenyi Biotec, Tokyo, Japan). Mouse IgG1 PE- and fluorescein-conjugated antibodies (R&D Systems, Minneapolis, MN, USA) were used as negative controls for anti-Vimentin PE and anti-EpCAM FITC, respectively. For staining the CD44 variant, anti-CD44v9 (Cosmo Bio, Tokyo, Japan) and mouse anti-rat IgG FITC (Thermo Fisher Scientific) were used as primary and secondary antibodies, respectively. Rat IgG2a, k Isotype Control (Thermo Fisher Scientific) was used as a negative control for the anti-CD44v9 antibody. Flow cytometric analysis was undertaken using a MACSQuant analyzer (Miltenyi Biotec).

2.7 | Quantitative real-time PCR

The expression levels of EMT-related genes were examined by quantitative real-time (qRT)-PCR as described previously, with minor modifications.²⁷ The qRT-PCR amplification was carried out using LightCycler 480 Probe Master (Roche Diagnostics, Tokyo, Japan) and Universal ProbeLibrary (Roche Diagnostics) probes in a LightCycler System (version 3; Roche Diagnostics). Primers and probes are listed in Table 1. Amplification was carried out according to a two-step cycle procedure consisting of 45 cycles of denaturation at 95°C for 10 seconds and annealing/elongation at 60°C for 30 seconds. The mRNA levels were measured semiquantitatively using the Δ/Δ threshold cycle (Ct) method. *GAPDH* and *PGK1* were used simultaneously as controls. Values are expressed relative to SK-HEP-1 cells. Triplicate wells were analyzed in each assay.

2.8 | Statistical analysis

Each experiment was repeated at least three times. Data are expressed as means \pm SD. Significant differences were evaluated by

TABLE 1 Primers and hydrolysis probes used in this study

Gene	Sequence
<i>TWIST1</i>	
5'-primer	5'-CGGCCAGGTACATCGACT-3'
3'-primer	5'-CATCTTGGAGTCCAGCTCGT-3'
Hydrolysis probe	UPL Probe #65 ^a
<i>TWIST2</i>	
5'-primer	5'-GCAAGAAGTCGAGCGAAGAT-3'
3'-primer	5'-GCTCTGCAGCTCCTCGAA-3'
Hydrolysis probe	UPL Probe #45 ^a
<i>SNAI1</i>	
5'-primer	5'-CATGTCCGGACCCACACT-3'
3'-primer	5'-TGGCACTGGTACTTCTTGACA-3'
Hydrolysis probe	UPL Probe #10 ^a
<i>SNAI2</i>	
5'-primer	5'-TGGTTGCTTCAAGGACACAT-3'
3'-primer	5'-GTTGCAGTGAGGGCAAGAA-3'
Hydrolysis probe	UPL Probe #7 ^a
<i>SNAI3</i>	
5'-primer	5'-TGCAAGATCTGTGGCAAGG-3'
3'-primer	5'-CAGTGCAGCAGGCATAG-3'
Hydrolysis probe	UPL Probe #80 ^a
<i>ZEB1</i>	
5'-primer	5'-CCTAAAAGAGCACTTAAGAATTCACAG-3'
3'-primer	5'-CATTCTTACTGCTTATGTGTGAGC-3'
Hydrolysis probe	UPL Probe #36 ^a
<i>ZEB2</i>	
5'-primer	5'-AAGCCAGGGACAGATCAGC-3'
3'-primer	5'-CCACACTCTGTGCATTTGAACT-3'
Hydrolysis probe	UPL Probe #68 ^a
<i>HMGA2</i>	
5'-primer	5'-TCCCTCTAAAGCAGCTCAAAA-3'
3'-primer	5'-ACTTGTGTGGCCATTTCT-3'
Hydrolysis probe	UPL Probe #34 ^a
<i>GAPDH</i>	
5'-primer	5'-AGCCACATCGCTCAGACAC-3'
3'-primer	5'-GCCCAATACGACCAATCC-3'
Hydrolysis probe	UPL Probe #60 ^a
<i>PGK1</i>	
5'-primer	5'-CTGTGGCTTCTGGCATACT-3'
3'-primer	5'-CGAGTGACAGCCTCAGCATA-3'
Hydrolysis probe	UPL Probe #42 ^a

^aUniversal ProbeLibrary (UPL) probe number (Roche Diagnostics, Tokyo, Japan).

Fisher's exact test, or Student's or Welch's t -test, using R version 3.4.0 software (the R project website, <http://www.r-project.org/>). A P value <0.05 was considered statistically significant.

3 | RESULTS

3.1 | Ability of CSLCs to metastasize to the liver

We examined the liver metastatic potential of induced CSLC SK-sphere cells (Figure 1). NRG mice injected with 1×10^3 SK-sphere cells into the spleen showed an increased frequency of liver tumors compared to injection of the same number of parental SK-HEP-1

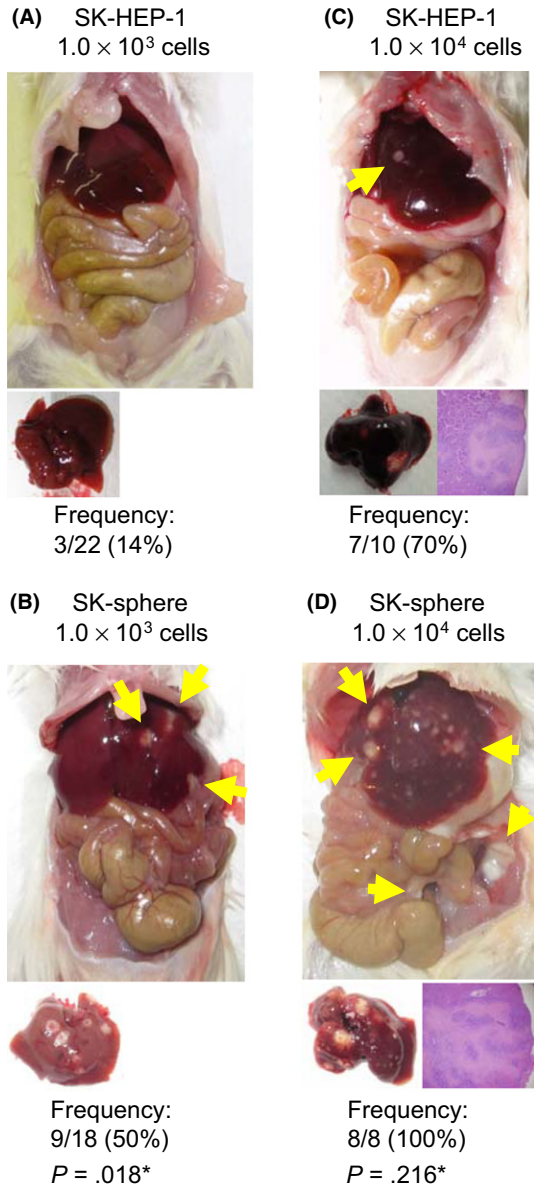


FIGURE 1 Liver metastasis ability of induced cancer stem-like cells. The metastatic ability of cells was evaluated by splenic injection into NOD-*Rag1*^{null} IL2 γ ^{null} double mutant mice. A,B, In mice injected with 1×10^3 SK-sphere or SK-HEP-1 cells, liver tumors were formed with a frequency of 9/18 (50%) and 3/22 (14%), respectively ($P = .018$). C,D, There is no significant difference in liver metastatic frequency in mice injected with 1×10^4 cells ($P = .216$). However, tumor areas were larger in SK-sphere- than in SK-HEP-1-injected mice. Yellow arrows indicate formed tumors. * $P < .05$ by Fisher's exact test

cells ($P < .05$). Peritoneal dissemination was observed in 4/18 (22%) of the SK-sphere cell-injected mice and 0/22 (0%) of the SK-HEP-1 cell-injected mice ($P < .05$). There was no difference in the frequency of liver tumors after injection of 1×10^4 cells. However, the areas occupied by the tumor in the cut surface of the livers were significantly increased in mice injected with SK-sphere cells compared to SK-HEP-1 cells ($57 \pm 26\%$ vs $10 \pm 3.4\%$, $P < .05$).

3.2 | Comprehensive mRNA expression analysis in CSLCs

Using quantitative RNA-seq analysis, we measured the comprehensive mRNA levels in both SK-sphere and parental SK-HEP-1 cells. After normalization, the mRNA expression profiles differed between SK-sphere, parental SK-HEP-1, and non-sphere forming HuH-7 cells (Figure 2A). There were 2067 genes with significant differences in the read counts between SK-sphere and SK-HEP-1 cells (fold change >2.0 ; q -value <0.05 ; 1328 upregulated and 739 downregulated genes) (Figure 2B, magenta dots). Considering the mRNA levels in HuH-7 cells that had no sphere-forming potential, 657 genes (518 upregulated and 139 downregulated) remained as specific differentially expressed genes in SK-sphere cells (Figure 2B, green dots). Gene set enrichment analysis with the mRNA expression profiles of SK-sphere and SK-HEP-1 cells showed there were significantly enriched signatures of tumor necrosis factor- α (TNF- α) signaling by nuclear factor- κ B (NF- κ B)-, hypoxia-, and EMT-related genes in SK-sphere cells (Figure 3; Table S1).

3.3 | Expression of EMT-related genes in CSLCs

The expression of EMT-related genes was examined by flow cytometry and qRT-PCR. Cells that were positive at the protein level for the mesenchymal marker, Vimentin, and negative for the epithelial marker, EpCAM, increased from 19.9% in SK-HEP-1 cells to 36.3% in SK-sphere cells (Figure 4). Interestingly, 94.9% of the Vimentin-positive cells were also CD44v9-positive (Figure S1). Similarly, among EMT-initiating transcription factors, mRNA levels of *TWIST1* and *SNAI1* were 2.2- and 60.7-fold higher in SK-sphere compared to SK-HEP-1 cells, respectively ($P < .05$; Figure 5). *HMG2* mRNA was also significantly upregulated in SK-sphere cells compared to parental cells ($P < .05$; Figure 5).

3.4 | Proportions of CD44 variant isoforms expressed in CSLCs

There are several isoform variants of CD44, which is a well-known cancer stem cell marker (Figure 6A). We evaluated the expression of each CD44 isoform variant in detail (Figure 6B). Fragments per kilobase of transcript per million (FPKM) values of the standard CD44 isoform in SK-sphere cells was downregulated 0.6-fold compared to parental cells. Conversely, FPKM values of CD44v8-10 were upregulated 2.9-fold. Interestingly, the FPKM value of the CD44 isoform containing the short cytoplasmic domain was more upregulated in sphere

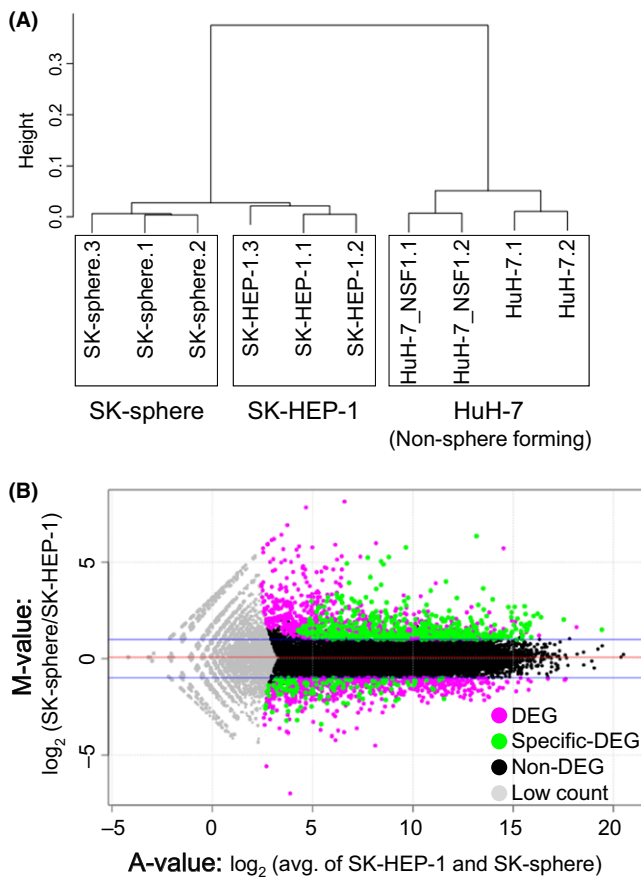
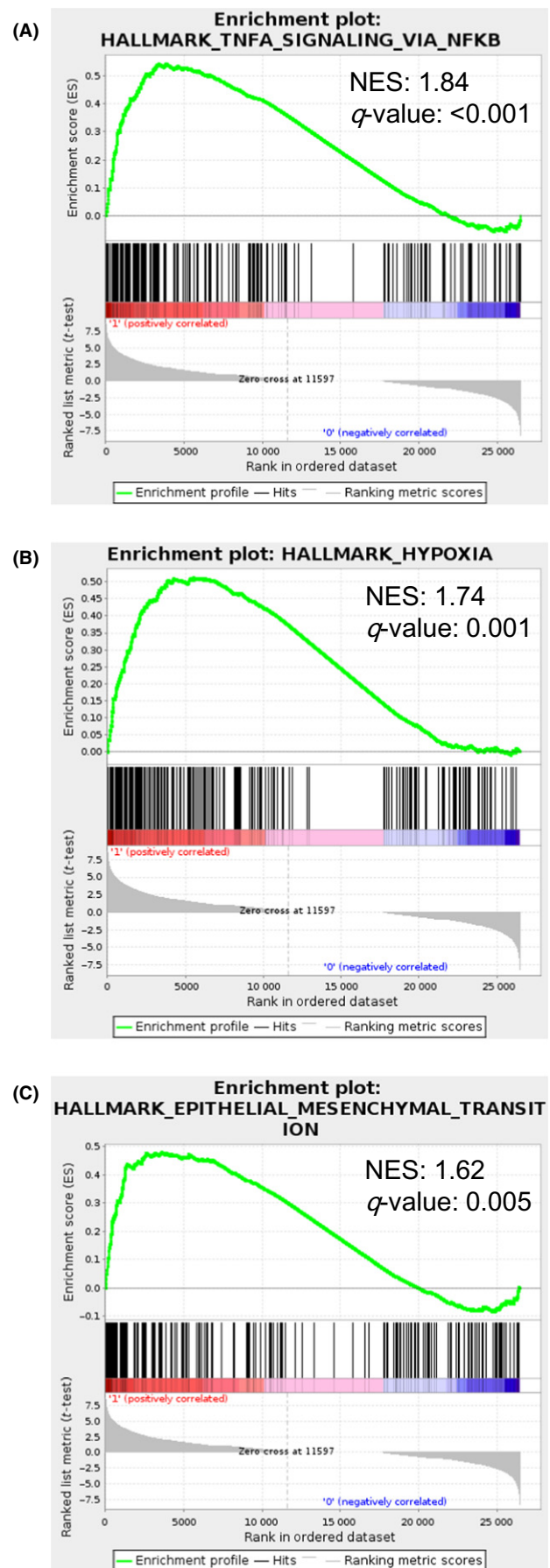


FIGURE 2 Clustering dendrogram and MA plot generated from RNA-sequencing analysis of cancer stem-like cells. A, Hierarchical clustering dendrogram of cells. Height is the Spearman distance between nodes consisting of three independent SK-HEP-1 and SK-sphere samples, and two independent samples of HuH-7 cells cultured in normal medium and sphere-induction medium containing neural survival factor-1. B, MA plot of RNA-sequencing read count data for SK-sphere vs SK-HEP-1 cells. For each gene, the \log_2 (average expression) in the two samples (A, x axis) against the \log_2 (fold change) between the samples is plotted (M, y axis). Magenta and green circles represent significant differentially expressed genes (DEGs) between SK-sphere and SK-HEP-1 cells. Genes indicated by green circles are sphere-specific DEGs that were not significantly changed in the experiment using non-sphere forming HuH-7 cells. Black circles are genes that are not significantly different between SK-sphere and SK-HEP-1 cells. Gray circles are genes with low expression counts in both SK-sphere and SK-HEP1 cells. Horizontal red and blue lines indicate the median of the M-value and cut-off of fold change, respectively

FIGURE 3 Enriched molecular signatures in cancer stem-like cells. RNA-sequencing data obtained from SK-sphere and SK-HEP-1 cells were subjected to Gene Set Enrichment Analysis. Enrichment plots from Gene Set Enrichment Analysis data show significant enrichment of tumor necrosis factor- α (TNF- α) signaling through nuclear factor- κ B (NF- κ B) (A), hypoxia (B), and epithelial-mesenchymal transition (C) genes in SK-sphere cells relative to SK-HEP-1 cells ($q < 0.01$). NES, normalized enrichment score



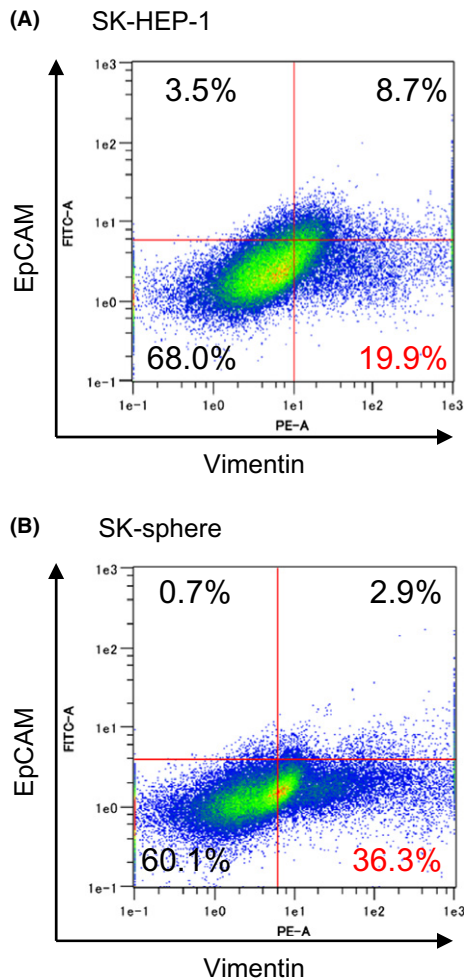


FIGURE 4 Flow cytometric analysis of Vimentin expression in cancer stem-like cells. Cells were stained with phycoerythrin (PE)-conjugated anti-Vimentin and FITC-conjugated anti-epithelial cell adhesion molecule (EpCAM) antibodies, and separated by flow cytometry. SK-sphere cells, as induced cancer stem-like cells, show an increased population of Vimentin-positive and EpCAM-negative cells compared to parental SK-HEP-1 cells (36.3% vs 19.9%)

cells compared to CD44v8-10 (8.8-fold). Expression of the CD44 short-tail variant isoform relative to all CD44 variants was 1.0% in parental SK-HEP-1 cells, but increased to 11.7% in SK-sphere cells. Expression of the CD44v8-10 isoforms relative to all variants was increased to 1.4% in SK-sphere cells compared to 0.4% in SK-HEP-1 cells. Moreover, the proportion of CD44 short-tail isoforms were also increased in surgically resected specimens obtained from hepatocellular carcinoma (HCC) patients with poor prognosis compared to those with long-term recurrence-free survival (Figure S2).

4 | DISCUSSION

In the present study, we examined the metastatic phenotype of induced sphere CSLCs from a hepatoma. Injecting SK-sphere cells into immune-deficient mice resulted in increased liver metastasis compared to parental SK-HEP-1 cells (Figure 1). Consistent with the enriched expression of

EMT- and hypoxia-related genes in SK-sphere cells, expression of an EMT marker, Vimentin, and EMT-related transcription factors, was upregulated in SK-sphere cells. In addition, expression analysis of CD44 variant isoforms revealed a decreased proportion of the standard CD44 isoform in SK-sphere cells. In contrast, expression of the variant isoforms of CD44 was increased in SK-sphere cells.

In this splenic injection model, CSLCs must survive in the bloodstream, migrate from blood vessels to the liver, and form a tumor in the internal organ environment.²⁸ This process is similar to hematogenous metastasis in clinical practice. In contrast, an s.c. injection model showed no significant difference of tumorigenicity between induced CSLCs and parental cells (unpublished data). It was reported that liver-CSC marker CD133⁺ cells had high self-renewal and tumorigenic capacity compared to CD133⁻ cells.^{29,30} Although the tumorigenic ability through s.c. injection was identified as one of the CSC characteristics, there was no difference in tumor-forming rates by s.c. injection between cancer stem-like CD44⁺/CD24^{-/low} breast cancer cells induced by EMT-inducing cytokines and parental cells without cytokine exposure.³¹ Interestingly, our CSLCs revealed CD133⁻/CD44^{high}/CD24^{low} expression, unlike typical liver CSCs.¹²

Consistent with the finding in the current study that the expression of EMT-related genes was increased in CSLCs (Figure 3C), several previous studies reported that enhancement of the EMT correlated to the metastatic potential and CSC state.³²⁻³⁸ Indeed, the proportion of cells positive for the mesenchymal marker, Vimentin, and the expression of the EMT-promoting transcription factors Twist1 and Snail, were increased in CSLCs (Figures 4,5).

High mobility group AT-hook 2 (HMGA2), which is a target for *let-7a-5p* microRNA, is associated with high rates of metastasis, poor prognosis, and induction of the EMT in several cancers, including hepatoma.³⁹⁻⁴¹ We observed a reduced level of *let-7a-5p* microRNA and an elevated HMGA2 protein level in SK-sphere cells by microarray and iTRAQ-labeled 2-D liquid chromatography-tandem mass spectrometry analyses, respectively (unpublished data). Elevated HMGA2 levels were confirmed by qPCR analysis (Figure 5). Overall, our results support that EMT enhances the metastatic phenotype of CSCs, although our CSLCs differed from typical liver CSCs in CD133 expression and s.c. tumorigenicity.

Hypoxia has been reported to cause drug resistance.^{42,43} RNA-sequencing followed by gene set enrichment analysis showed significant enrichment of not only EMT-related genes, but also hypoxia-related genes in CSLCs (Figure 3B). This result corresponded to our previous report that induced chemoresistant CSLCs expressed higher *HIF1A* mRNA levels.¹²

Gene Set Enrichment Analysis revealed that TNF- α signaling through the NF- κ B signature was also enriched in CSLCs (Figure 3A). In chronic myeloid leukemia stem cells and leukemia-initiating cells of acute myeloid leukemia, NF- κ B activity was promoted by TNF- α secretion.^{44,45} In addition, CD24^{-/low}/CD44⁺ breast CSCs, wherein TNF signaling was enhanced, possessed higher NF- κ B activity compared to non-CSCs.⁴⁶ The NF- κ B-dependent stabilization of Snail in several cancer cell lines by TNF- α treatment caused EMT, which in turn increased cell invasiveness.^{38,47}

FIGURE 5 Messenger RNA levels of epithelial-mesenchymal transition-promoting transcription factors in cancer stem-like cells. Expression levels of *TWIST1*, *TWIST2*, *SNAI1*, *SNAI2*, *ZEB1*, *ZEB2*, and *HMGA2* were measured with quantitative real-time PCR. Data are presented as ratios to levels in SK-HEP-1 hepatoma cells. Open and gray columns represent values from SK-HEP-1 and SK-sphere cells, respectively. **P* < .05 with Student's *t*-test or Welch's *t*-test

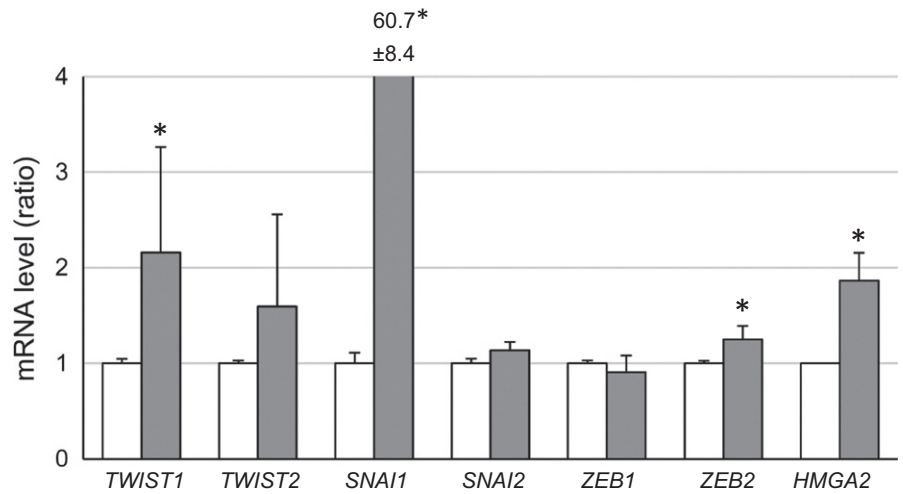
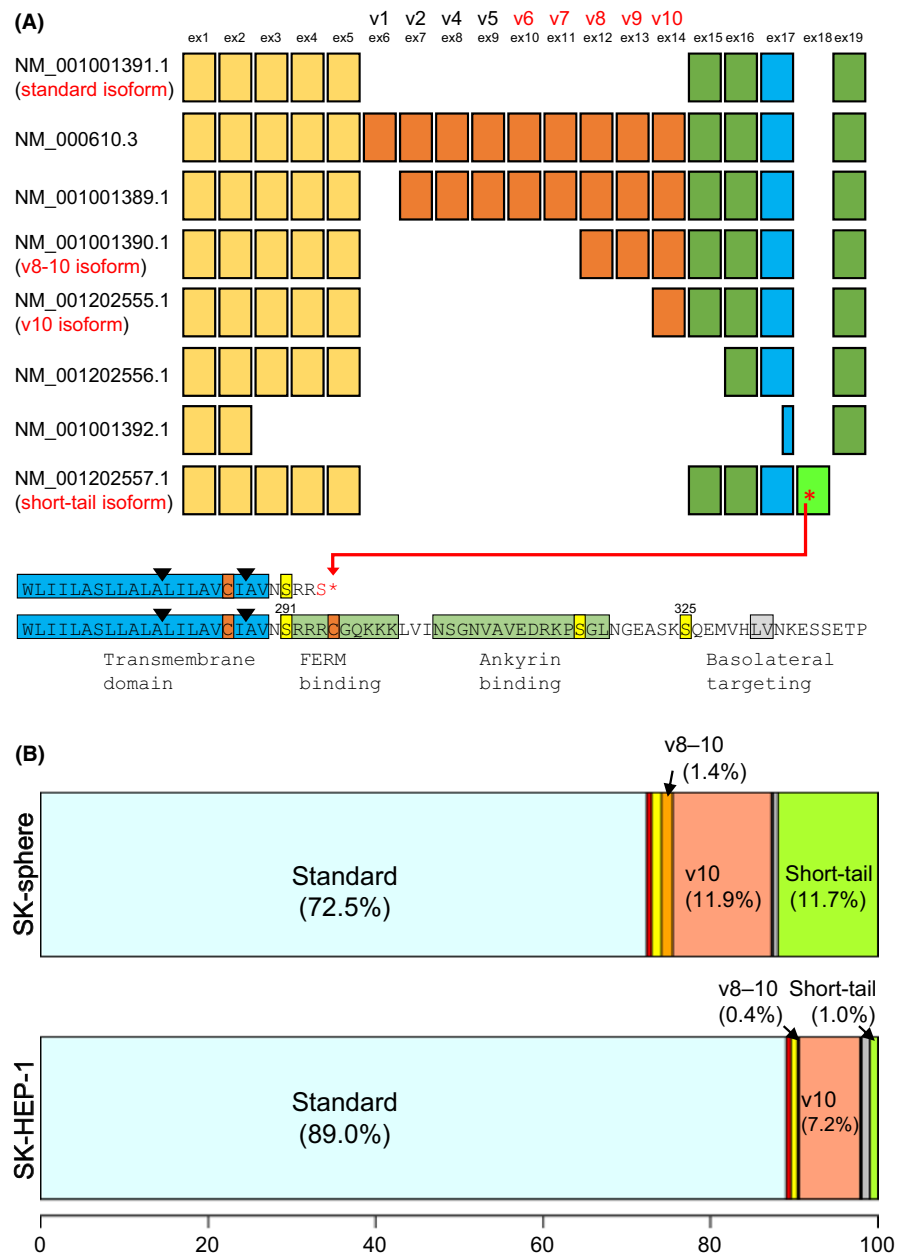


FIGURE 6 Expression of CD44 isoforms in cancer stem-like cells (SK-sphere) and parental cancer cells (SK-HEP-1). A, CD44 structure of mRNA splicing patterns according to the RefSeq database is shown. NM_001001391.1 is the standard form of CD44, CD44s. The variant (v) forms of CD44, CD44v1-10, contain extra exons (ex) as shown by the orange boxes. NM_001202557.1 contains exon 18 instead of exon 19, resulting in a short-tail isoform due to an alternative translation stop codon. Lower panel, amino acid sequence features of the transmembrane domain and several functional motifs are shown. An asterisk connected by a red arrow indicates a stop codon in exon 18 of the short-tail isoform. This differs from exon 19 of other isoforms represented below the sequence. Arrowheads represent sites for regulated intramembranous cleavage. Serine residues, that are phosphorylation sites, and cysteine residues, where palmitoylation occurs, are represented by yellow and orange, respectively. B, Bar plots showing the proportions of CD44 isoforms expressed in SK-HEP-1 and SK-sphere cells. The standard CD44 isoform (cyan) is decreased in SK-sphere (upper bar) compared to SK-HEP-1 cells (lower bar). In contrast to the significant decrease in the standard CD44 isoform, CD44v8-10 (orange), CD44v10 (salmon), and CD44 short-tail (green) isoforms are significantly increased in SK-sphere cells



In our previous study, CSLCs contained increased numbers of CD44v9⁺ cells.¹² CD44 variants are considered to be CSC markers of many cancers.⁴⁸ CD44 variants with an extra extracellular domain, such as CD44v9, are functionally associated with the chemoresistant phenotype of CSCs. CD44 variant isoforms bind and stabilize to the cystine transporter, xCT, in the cell membrane. The resulting production of glutathione, an antioxidant, enhances resistance to oxidative stress.^{49,50} Furthermore, CD44 variants increase the metastatic potential of rat pancreatic carcinoma cells.⁵¹ CD44v3, v8-10, and MMP9 can bind to each other on the cell surface. Those interactions lead to degradation of the ECM, which contributes to cell invasion and migration processes.⁵²

Interestingly, in addition to CD44v8-10 isoforms, induced CSLCs showed increased expression of a rare CD44 short-tail isoform (Figure 6). The CD44 short-tail isoform had not been of interest as a research target because of its very low abundance compared with other CD44 isoforms.^{53,54} Thus, there are few reports on the CD44 short-tail isoform, and its role in cancer and CSCs has been almost unknown. Among the few existing reports, it was shown that knockdown of the CD44 short-tail variant enhanced hyaluronan internalization and decreased cell-associated matrices in particular chondrocytes.⁵⁵ Moreover, HCCs with poor prognosis showed a greater proportion of the CD44 short-tail isoform than those with a good prognosis (Figure S2). Our RNA-seq data showed that mRNA levels of *GFPT1* (also known as *GFAT1*) encoding glutamine-fructose-6-phosphate transaminase 1, a hexosamine biosynthetic pathway rate-limiting enzyme, were significantly higher in both CSLCs (2.2-fold) and poor prognostic HCCs (1.8-fold) compared to parental cells and good prognostic HCCs, respectively (unpublished data). Inhibition of *GFPT1* by its antagonist decreased hexosamine biosynthetic pathway-dependent hyaluronic acid production, hypoxia-inducible factor-1 α signaling, and CD44^{high}/CD24^{low} breast CSLC populations.⁵⁶ Taken together, the CD44 short-tail isoform might be related to CSC properties through hyaluronan metabolism and/or signaling. Further studies are needed to identify the role of the CD44 short-tail isoform in CSCs.

In conclusion, our induced CSLCs possessed metastatic in addition to chemoresistant characteristics. The EMT, and CD44 variants, including the short-tail isoform as well as the v8-10 isoforms, might correlate with the CSC phenotype. The CSLCs used in this study might be responsible for the poor prognosis of human liver cancer; hence, further detailed investigations with the integration of CSLCs and clinical samples could disclose key therapeutic target genes for liver cancer.

ACKNOWLEDGMENTS

We appreciate the assistance provided by Akiko Sano for this project. This work was partly supported by the Japan Society for the Promotion of Science (KAKENHI grant nos. 16K10574, 25861192, and 24659610).

CONFLICT OF INTEREST

Shoichi Hazama and Hiroaki Nagano received research funds from Toyo Kohan Co., Ltd and NEC Corporation. Kiyoshi Yoshimura owns stock in Noile-Immune Biotech, Inc. The other authors have no conflict of interest.

ORCID

Ryouichi Tsunedomi  <http://orcid.org/0000-0003-4251-1936>
Shoichi Hazama  <http://orcid.org/0000-0002-5239-8570>

REFERENCES

1. Visvader JE. Cells of origin in cancer. *Nature*. 2011;469:314-322.
2. Visvader JE, Lindeman GJ. Cancer stem cells: current status and evolving complexities. *Cell Stem Cell*. 2012;10:717-728.
3. Botchkina G. Colon cancer stem cells—from basic to clinical application. *Cancer Lett*. 2013;338:127-140.
4. Yang Z, Ho D, Ng M, et al. Significance of CD90 + cancerstem cells in human liver cancer. *Cancer Cell*. 2008;13:153-166.
5. Brungs D, Aghmesheh M, Vine KL, Becker TM, Carolan MG, Ranson M. Gastric cancer stem cells: evidence, potential markers, and clinical implications. *J Gastroenterol*. 2016;51:313326.
6. Croker AK, Goodale D, Chu J, et al. High aldehyde dehydrogenase and expression of cancer stem cell markers selects for breast cancer cells with enhanced malignant and metastatic ability. *J Cell Mol Med*. 2009;13:2236-2252.
7. Haraguchi N, Ishii H, Mimori K, et al. CD13 is a therapeutic target in human liver cancer stem cells. *J Clin Invest*. 2010;120:3326-3339.
8. Mani SA, Guo W, Liao MJ, et al. The epithelial-mesenchymal transition generates cells with properties of stem cells. *Cell*. 2008;133:704-715.
9. Scheel C, Weinberg RA. Phenotypic plasticity and epithelial-mesenchymal transitions in cancer - and normal stem cells? *Int J Cancer*. 2011;129:2310-2314.
10. Watanabe Y, Yoshimura K, Yoshikawa K, et al. A stem cell medium containing neural stimulating factor induces a pancreatic cancer stem-like cell-enriched population. *Int J Oncol*. 2014;45:1857-1866.
11. Matsukuma S, Yoshimura K, Ueno T, et al. Calreticulin is highly expressed in pancreatic cancer stem-like cells. *Cancer Sci*. 2016;107:1599-1609.
12. Hashimoto N, Tsunedomi R, Yoshimura K, et al. Cancer stem-like sphere cells induced from de-differentiated hepatocellular carcinoma-derived cell lines possess the resistance to anti-cancer drugs. *BMC Cancer*. 2014;14:722.
13. Bruix J, Gores GJ, Mazzaferro V. Hepatocellular carcinoma: clinical frontiers and perspectives. *Gut*. 2014;63:844-855.
14. Forner A, Llovet JM, Bruix J. Hepatocellular carcinoma. *Lancet*. 2012;379:1245-1255.
15. Colvin H, Mizushima T, Eguchi H, Takiguchi S, Doki Y, Mori M. Gastroenterological surgery in Japan: the past, the present and the future. *Ann Gastroenterol Surg*. 2017;1:5-10.
16. Luzzi KJ, MacDonald IC, Schmidt EE, et al. Multistep nature of metastatic inefficiency: dormancy of solitary cells after successful extravasation and limited survival of early micrometastases. *Am J Pathol*. 1998;153:865-873.
17. van den Hoogen C, van der Horst G, Cheung H, et al. High aldehyde dehydrogenase activity identifies tumor-initiating and metastasis-initiating cells in human prostate cancer. *Cancer Res*. 2010;70:5163-5173.

18. Bhagwandin VJ, Bishop JM, Wright WE, Shay JW. The metastatic potential and chemoresistance of human pancreatic cancer stem cells. *PLoS ONE*. 2016;11:e0148807.
19. Pang R, Law W, Chu A, et al. A subpopulation of CD26 + cancer stem cells with metastatic capacity in human colorectal cancer. *Cell Stem Cell*. 2010;6:603-615.
20. Martin M. Cutadapt removes adapter sequences from high-throughput sequencing reads. *EMBnet J*. 2011;17:10-12.
21. Wang T, Liu J, Shen L, et al. STAR: an integrated solution to management and visualization of sequencing data. *Bioinformatics*. 2013;29:3204-3210.
22. Robinson M, Oshlack A. A scaling normalization method for differential expression analysis of RNA-seq data. *Genome Biol*. 2010;11:R25.
23. Sun J, Nishiyama T, Shimizu K, Kadota K. TCC: an R package for comparing tag count data with robust normalization strategies. *BMC Bioinformatics*. 2013;14:219.
24. Tang M, Sun J, Shimizu K, Kadota K. Evaluation of methods for differential expression analysis on multi-group RNA-seq count data. *BMC Bioinformatics*. 2015;16:361.
25. Subramanian A, Tamayo P, Mootha VK, et al. Gene set enrichment analysis: a knowledge-based approach for interpreting genome-wide expression profiles. *Proc Natl Acad Sci*. 2005;102:15545-15550.
26. Trapnell C, Williams BA, Pertea G, et al. Transcript assembly and quantification by RNA-Seq reveals unannotated transcripts and isoform switching during cell differentiation. *Nat Biotechnol*. 2010;28:511-515.
27. Tsunedomi R, Iizuka N, Tamesa T, et al. Decreased ID2 promotes metastatic potentials of hepatocellular carcinoma by altering secretion of vascular endothelial growth factor. *Clin Cancer Res*. 2008;14:1025-1031.
28. Yoshimura K, Meckel KF, Laird LS, et al. Integrin alpha2 mediates selective metastasis to the liver. *Cancer Res*. 2009;69:7320-7328.
29. Suetsugu A, Nagaki M, Aoki H, Motohashi T, Kunisada T, Moriwaki H. Characterization of CD133 + hepatocellular carcinoma cells as cancer stem/progenitor cells. *Biochem Biophys Res Commun*. 2006;351:820-824.
30. Yin S, Li J, Hu C, et al. CD133 positive hepatocellular carcinoma cells possess high capacity for tumorigenicity. *Int J Cancer*. 2007;20:1444-1450.
31. Xie G, Ji A, Yuan Q, et al. Tumour-initiating capacity is independent of epithelial-mesenchymal transition status in breast cancer cell lines. *Br J Cancer*. 2014;110:2514-2523.
32. Christiansen JJ, Rajasekaran AK. Reassessing epithelial to mesenchymal transition as a prerequisite for carcinoma invasion and metastasis. *Cancer Res*. 2006;66:8319-8326.
33. Moore LD, Isayeva T, Siegal GP, Ponnazhagan S. Silencing of transforming growth factor-beta1 in situ by RNA interference for breast cancer: implications for proliferation and migration in vitro and metastasis in vivo. *Clin Cancer Res*. 2008;14:4961-4970.
34. Kudo-Saito C, Shirako H, Takeuchi T, Kawakami Y. Cancer metastasis is accelerated through immunosuppression during Snail-induced EMT of cancer cells. *Cancer Cell*. 2009;15:195-206.
35. Gibbons D, Lin W, Creighton C, et al. Contextual extracellular cues promote tumor cell EMT and metastasis by regulating miR-200 family expression. *Genes Dev*. 2009;23:2140-2151.
36. Chaffer CL, Weinberg RA. A perspective on cancer cell metastasis. *Science*. 2011;331:1559-1564.
37. Liu X, Fan D. The epithelial-mesenchymal transition and cancer stem cells: functional and mechanistic links. *Curr Pharm Des*. 2015;21:1279-1291.
38. Shibue T, Weinberg RA. EMT, CSCs, and drug resistance: the mechanistic link and clinical implications. *Nat Rev Clin Oncol*. 2017;14:611-629.
39. Wu J, Zhang S, Shan J, et al. Elevated HMGA2 expression is associated with cancer aggressiveness and predicts poor outcome in breast cancer. *Cancer Lett*. 2016;376:284-292.
40. Morishita A, Zaidi MR, Mitoro A, et al. HMGA2 is a driver of tumor metastasis. *Cancer Res*. 2013;73:4289-4299.
41. Luo Y, Li W, Liao H. HMGA2 induces epithelial-to-mesenchymal transition in human hepatocellular carcinoma cells. *Oncol Lett*. 2013;5:1353-1356.
42. Shannon AM, Bouchier-Hayes DJ, Condrón CM, Toomey D. Tumour hypoxia, chemotherapeutic resistance and hypoxia-related therapies. *Cancer Treat Rev*. 2003;29:297-307.
43. Song X, Liu X, Chi W, et al. Hypoxia-induced resistance to cisplatin and doxorubicin in non-small cell lung cancer is inhibited by silencing of HIF-1alpha gene. *Cancer Chemother Pharmacol*. 2006;58:776-784.
44. Gallipoli P, Pellicano F, Morrison H, et al. Autocrine TNF- α production supports CML stem and progenitor cell survival and enhances their proliferation. *Blood*. 2013;122:3335-3339.
45. Kagoya Y, Yoshimi A, Kataoka K, et al. Positive feedback between NF- κ B and TNF- α promotes leukemia-initiating cell capacity. *J Clin Invest*. 2014;124:528-542.
46. Murohashi M, Hinohara K, Kuroda M, et al. Gene set enrichment analysis provides insight into novel signalling pathways in breast cancer stem cells. *Br J Cancer*. 2010;102:206-212.
47. Wu Y, Deng J, Rychalou PG, Qiu S, Evers BM, Zhou BP. Stabilization of snail by NF-kappaB is required for inflammation-induced cell migration and invasion. *Cancer Cell*. 2009;15:416-428.
48. Yan Y, Zuo X, Wei D. Concise review: emerging role of CD44 in cancer stem cells: a promising biomarker and therapeutic target. *Stem Cells Transl Med*. 2015;4:1033-1043.
49. Ishimoto T, Nagano O, Yae T, et al. CD44 variant regulates redox status in cancer cells by stabilizing the xCT subunit of system xc- and thereby promotes tumor growth. *Cancer Cell*. 2011;19:387-400.
50. Nagano O, Okazaki S, Saya H. Redox regulation in stem-like cancer cells by CD44 variant isoforms. *Oncogene*. 2013;32:5191-5198.
51. Gunthert U, Hofmann M, Rudy W, et al. A new variant of glycoprotein CD 44 confers Metastatic potential to rat carcinoma cells. *Cell*. 1991;65:13-24.
52. Yu Q, Stamenkovic I. Localization of matrix metalloproteinase 9 to the cell surface provides a mechanism for CD 44-mediated tumor invasion. *Genes Dev*. 1999;13:35-48.
53. Goldstein LA, Zhou DF, Picker LJ, et al. A human lymphocyte homing receptor, the Hermes antigen, is related to cartilage proteoglycan core and link proteins. *Cell*. 1989;56:1063-1072.
54. Goldstein LA, Butcher EC. Identification of mRNA that encodes an alternative form of H-CAM (CD44) in lymphoid and nonlymphoid tissues. *Immunogenetics*. 1990;32:389-397.
55. Jiang H, Knudson C, Knudson W. Antisense inhibition of CD44 tail-less splice variant in human articular chondrocytes promotes hyaluronan internalization. *Arthritis Rheum*. 2001;44:2599-2610.
56. Chanmee T, Ontong P, Izumikawa T, et al. Hyaluronan production regulates metabolic and cancer stem-like properties of breast cancer cells via hexosamine biosynthetic pathway-coupled HIF-1 signaling. *J Biol Chem*. 2016;291:24105-24120.

SUPPORTING INFORMATION

Additional Supporting Information may be found online in the supporting information tab for this article.

How to cite this article: Nishiyama M, Tsunedomi R, Yoshimura K, et al. Metastatic ability and the epithelial-mesenchymal transition in induced cancer stem-like hepatoma cells. *Cancer Sci*. 2018;109:1101-1109. <https://doi.org/10.1111/cas.13527>